Nuclear Physics B331 (1990) 515–530
North-Holland

NUMERICAL SIMULATION OF THE O(4)-SYMMETRIC ϕ^4-MODEL IN THE SYMMETRIC PHASE

Ch. FRICK[a], K. JANSEN[b], J. JERSÁK[a,b], I. MONTVAY[c], G. MÜNSTER[d] and P. SEUFERLING[c]

[a] *Institut für Theoretische Physik E, Technische Hochschule Aachen, D-5100 Aachen, FRG*
[b] *HLRZ c/o KFA, P.O. Box 1913, D-5170 Jülich, FRG*
[c] *Deutsches Elektronen-Synchrotron DESY, Notkestr. 85, D-2000 Hamburg 52, FRG*
[d] *II. Institut für Theoretische Physik der Universität Hamburg, Luruper Chaussee 149, D-2000 Hamburg 50, FRG*

Received 18 July 1989

The four-dimensional O(4)-symmetric ϕ^4-model is numerically simulated on lattices $L^3 \cdot T$ with $4 \leqslant L \leqslant 16$ and $T = 12, 16$ in the phase with unbroken symmetry at infinite bare quartic coupling. Physical observables, such as the renormalized mass and coupling, are determined with good precision by using a recently developed efficient cluster algorithm. Special care is taken to study the finite volume dependence in order to achieve a reliable infinite volume extrapolation. The finite volume behaviour of masses and couplings is well approximated by one-loop renormalized perturbation theory. The obtained infinite volume results agree with a recent analytical calculation based on a high-order hopping parameter expansion.

1. Introduction

The numerical simulation of four-dimensional scalar field theories with quartic coupling ("ϕ^4-theory") has recently received a lot of interest. The theory with a 4-component scalar field in the phase with spontaneously broken O(4) symmetry is the basis of the Higgs sector of the standard model, therefore it has an immediate physical relevance. Assuming that the influence of the Yukawa couplings of the fermions is small and that the gauge interactions can be dealt with in perturbation theory [1, 2], one can obtain a non-perturbative upper bound on the mass of the physical Higgs boson [3–7].

More generally, the numerical simulation of four-dimensional ϕ^4-theories is of intrinsic theoretical interest, because these are the simplest examples of four-dimensional renormalizable quantum field theories which can be fully understood by using non-perturbative analytical and numerical methods. Many interesting theoretical phenomena can be studied in detail and with sufficient precision in ϕ^4-models. Several authors of our present collaboration recently performed a series of investigations in the Ising limit (i.e. infinitely strong quartic self-coupling limit) of the

0550-3213/90/$03.50

one-component ϕ^4-model [8,9] which has many qualitatively similar features as the O(4) model, but also has some peculiarities, like e.g. vacuum tunnelling, having their own theoretical implications. In the present article we shall numerically study the O(4)-symmetric phase of the 4-component ϕ^4-model at infinite bare quartic coupling (fixed length of the scalar field) in the same spirit as refs. [8,9], namely paying special attention to the finite volume behaviour of the measurable physical quantities. In addition, similarly to the one-component case, we can compare the infinite volume extrapolation of the physical quantities to the results of the non-perturbative analytical work of Lüscher and Weisz [7].

In order to achieve sufficient precision in the simulation it is important to have an efficient numerical algorithm, if in particular one tries to determine quantities which involve a lot of cancellation as, for instance, the very important renormalized coupling. Recently new cluster algorithms for continuous spin models were invented by Niedermayer [10] and Wolff [11]. After starting this calculation on the smaller ($T = 12$) lattices by the conventional local Metropolis algorithm three members of our collaboration implemented and tested the non-local cluster algorithms, which were used previously in lower-dimensional models, in the four-dimensional O(4) ϕ^4-model. The results of this investigation [12] showed that the "reflection cluster algorithm" of Wolff is the most efficient one. This is due to the fact that besides fighting critical slowing down it also allows for variance reduction in important measurable quantities. The gain in computer time for achieving the same precision is of the order of a factor of 10–100, therefore we performed the $T = 16$ runs with the reflection cluster algorithm and added a 12^4 run with this algorithm to the previous statistics.

The plan of this paper is as follows: in sect. 2 basic definitions will be collected and the one-loop perturbative formulae for the volume dependence of the renormalized mass and couplings will be given. In addition, the connection of the two-particle energies with the scattering lengths in the appropriate channels is discussed following ref. [13]. Sect. 3 is devoted to the presentation and discussion of the numerical results. The summary and conclusions are in sect. 4.

2. Basic formulae and perturbation theory

In this section we consider the theory of a real N-component scalar field ϕ_x^α, $\alpha = 1, \ldots, N$. We keep N arbitrary although in the numerical calculations discussed below $N = 4$ always. On a hypercubical lattice $\mathbb{Z}^4$ in four dimensions the O(N)-symmetric action of ϕ^4-theory is parametrized as

$$S = \sum_x \left\{ -2\kappa \sum_{\mu=1}^{4} \phi_x \cdot \phi_{x+\hat{\mu}} + \phi_x \cdot \phi_x + \lambda (\phi_x \cdot \phi_x - 1)^2 \right\}, \tag{1}$$

where the lattice spacing a is set to 1 and $\hat{\mu}$ denotes the unit vector in the positive μ-direction. The O(N)-symmetric non-linear sigma model is characterized by the additional restriction of a fixed length for the field

$$\phi_x \cdot \phi_x = 1 \tag{2}$$

and is equivalent to the ϕ^4-theory in the limit of an infinite bare quartic self-coupling $\lambda = \infty$. In the following, however, we also allow finite values of λ.

For values of κ below a certain critical κ_c the O(N) symmetry is unbroken and the Green functions

$$G_{\alpha_1,\ldots,\alpha_n}(x_1,\ldots,x_n) = \frac{1}{Z}\int \prod_{x,\alpha} \mathrm{d}\phi_x^\alpha \, \mathrm{e}^{-S} \phi_{x_1}^{\alpha_1} \ldots \phi_{x_n}^{\alpha_n}$$

$$\equiv \langle \phi_{x_1}^{\alpha_1} \ldots \phi_{x_n}^{\alpha_n} \rangle \tag{3}$$

are O(N)-symmetric. The spectrum has a gap m corresponding to the mass of an O(N) vector multiplet of particles. This mass is given by the pole of the propagator closest to the origin. Let $\tilde{G}_{\alpha\beta}(p)$ be the propagator in momentum space. Then

$$\tilde{G}(p)^{-1}_{\alpha\beta} = 0, \qquad p = (im, 0, 0, 0). \tag{4}$$

The renormalized mass m_R and the wave function renormalization Z_R on the other hand are defined through the small momentum behaviour of the propagator:

$$\tilde{G}(p)^{-1}_{\alpha\beta} = 2\kappa Z_R^{-1} \delta_{\alpha\beta}\{ m_R^2 + p^2 + \mathcal{O}(p^4)\}. \tag{5}$$

The renormalized and the unrenormalized vertex functions are related through

$$\Gamma_R^{(n)}(p_1,\ldots,p_n)_{\alpha_1,\ldots,\alpha_n} = \left(2\kappa Z_R^{-1}\right)^{-n/2} \Gamma^{(n)}(p_1,\ldots,p_n)_{\alpha_1,\ldots,\alpha_n}. \tag{6}$$

The renormalized coupling g_R is defined in terms of the renormalized 4-point vertex function by

$$\Gamma_R^{(4)}(0,0,0,0)_{\alpha\beta\gamma\delta} = -g_R S_{\alpha\beta\gamma\delta}, \tag{7}$$

where

$$S_{\alpha\beta\gamma\delta} = \tfrac{1}{3}\left(\delta_{\alpha\beta}\delta_{\gamma\delta} + \delta_{\alpha\gamma}\delta_{\beta\delta} + \delta_{\alpha\delta}\delta_{\beta\gamma}\right). \tag{8}$$

As mentioned in sect. 1 we shall compare results from the Monte Carlo calculation with predictions from perturbation theory in sect. 3. Since the four-dimensional non-linear sigma model is a perturbatively non-renormalizable field theory the reader might wonder how perturbation theory can be applied. This is possible in the

following way. For finite bare coupling λ renormalized perturbation theory can be applied to the N-component ϕ^4-theory. This means that physical quantities are expanded in powers of the renormalized coupling g_R, the coefficients depending on the renormalized mass m_R. Renormalized perturbation theory can be successfully used near the critical point where the renormalized coupling becomes small. Outside this scaling region non-perturbative effects dominate.

The bare coupling and the renormalized coupling are numerically quite different. In particular g_R remains finite even in the limit where λ goes to infinity, which yields the non-linear sigma model. This gives us the possibility to apply renormalized perturbation theory in this case too. In this limit the coupling g_R and the mass m_R are related in a certain way, which cannot be calculated within perturbation theory. If, however, for a given g_R one knows the value of m_R from other sources one may use this as an input to the perturbative formulae.

In this article renormalized perturbation theory is applied to the volume dependence of physical quantities. We consider a lattice with spatial volume L^3 and euclidean time extent $T = \infty$, and with periodic boundary conditions. For fixed bare parameters κ and λ any renormalized quantity such as m, m_R or g_R will depend on L. We impose the renormalization conditions at $L = \infty$ which means that we identify

$$g_R \equiv g_R(\infty), \qquad m_R \equiv m_R(\infty) \tag{9}$$

as the renormalized parameters. The finite L deviations

$$\delta X(L) = X(L) - X(\infty) \tag{10}$$

for various quantities X can then be calculated in perturbation theory as power series in g_R. In the one-loop approximation the following loop integrals occur:

$$J_n(m_R, L) = \frac{1}{L^3} \sum_{\mathbf{k}} \int_{-\pi}^{\pi} \frac{\mathrm{d}k_4}{(2\pi)} \left(\hat{k}^2 + m_R^2\right)^{-n}, \tag{11}$$

where the sum over $\mathbf{k}$ goes over the Brillouin zone

$$k_i = \frac{2\pi}{L} n_i, \qquad n_i = 0, 1, 2, \ldots, L-1, \qquad i = 1, 2, 3 \tag{12}$$

and

$$\hat{k}_\mu = 2 \sin \tfrac{1}{2} k_\mu .$$

The results are

$$\delta m_{\mathrm{R}} = \frac{g_{\mathrm{R}}}{4m_{\mathrm{R}}} \frac{N+2}{3} \delta J_1 + \mathcal{O}\left(g_{\mathrm{R}}^2\right),$$

$$\delta m = \frac{g_{\mathrm{R}}}{4m_{\mathrm{R}}\sqrt{1+m_{\mathrm{R}}^2/4}} \frac{N+2}{3} \delta J_1 + \mathcal{O}\left(g_{\mathrm{R}}^2\right),$$

$$\delta g_{\mathrm{R}} = -\tfrac{3}{2} g_{\mathrm{R}}^2 \frac{N+8}{9} \delta J_2 + \mathcal{O}\left(g_{\mathrm{R}}^3\right),$$

$$\Delta Z_{\mathrm{R}} \equiv \frac{Z_{\mathrm{R}}(L)}{Z_{\mathrm{R}}(\infty)} - 1 = \mathcal{O}\left(g_{\mathrm{R}}^2\right), \tag{13}$$

where

$$\delta J_n \equiv J_n(m_{\mathrm{R}}, L) - J_n(m_{\mathrm{R}}, \infty).$$

Furthermore the mass m in the infinite volume is given by

$$m(\infty) = 2\log\left(\sqrt{1+m_{\mathrm{R}}^2/4} + \tfrac{1}{2} m_{\mathrm{R}}\right) + \mathcal{O}\left(g_{\mathrm{R}}^2\right). \tag{14}$$

Also particularly interesting are the masses of two-particle states. The leading finite volume corrections for two-particle masses are due to scattering effects and can be expressed in terms of the S-wave scattering length a_0 as has been shown by Lüscher [13]. For a two-particle state with zero relative momentum and mass M the shift due to the finite volume is given by

$$M(L) - 2m(L) = -\frac{4\pi a_0}{m_* L^3}\left(1 + c_1 \frac{a_0}{L} + c_2\left(\frac{a_0}{L}\right)^2\right) + \mathcal{O}(L^{-6}), \tag{15}$$

with the kinetic mass

$$m_* = \sinh m + \mathcal{O}\left(g_{\mathrm{R}}^2\right) \tag{16}$$

and constants

$$c_1 = -2.837297, \qquad c_2 = 6.375183. \tag{17}$$

A precise determination of the volume dependence of two-particle masses would thus allow us to obtain information about the scattering length.

We consider O(N) scalar and tensor two-particle states with zero relative momentum. They are created from the vacuum by the operator

$$S^{\alpha\beta}(t) = L^{-3} \sum_{x,\, y} \phi_x^\alpha \phi_y^\beta, \qquad x = (t, \boldsymbol{x}),\ y = (t, \boldsymbol{y}). \tag{18}$$

Taking the trace in α and β yields a scalar state, whereas the traceless part yields a tensor multiplet. The corresponding masses in the case $N = 4$ are denoted M_1 and M_9, where the index equals the dimension of the O(4) representation.

The scalar and tensor S-wave scattering lengths a_0^{s} and a_0^{t} have been calculated by Lüscher and Weisz [7] in two-loop perturbation theory in the continuum:

$$a_0^{\mathrm{s}} = -\frac{N+2}{6}\frac{\alpha_{\mathrm{R}}\pi}{m_*}\left\{1 - \frac{N+2}{3}\alpha_{\mathrm{R}} + \left(\frac{N^2}{9} + 0.34325N + 0.47133\right)\alpha_{\mathrm{R}}^2\right\}, \tag{19}$$

$$a_0^{\mathrm{t}} = -\frac{1}{3}\frac{\alpha_{\mathrm{R}}\pi}{m_*}\left\{1 - \tfrac{2}{3}\alpha_{\mathrm{R}} + (0.027637N + 0.47133)\alpha_{\mathrm{R}}^2\right\}, \tag{20}$$

where

$$\alpha_{\mathrm{R}} = g_{\mathrm{R}}/16\pi^2. \tag{21}$$

We shall use these expressions later to compare the results from the Monte Carlo calculations with the perturbative predictions.

We have calculated the two-particle masses M_1 and M_9 also directly in leading order perturbation theory on a lattice. The results agree with Lüscher's formula as expected.

For two-particle states with relative momentum

$$\boldsymbol{p} = \frac{2\pi}{L}\boldsymbol{n}, \qquad \boldsymbol{n} \in \mathbb{Z}^3 \tag{22}$$

the dominant finite volume effect

$$M(L) = 2m + \frac{4\pi^2 \boldsymbol{n}^2}{mL^2} + \mathcal{O}(L^{-3}) \tag{23}$$

is of purely kinematical origin. This case will not be considered here.

Another quantity which is considered in this article is the six-point coupling h_{R}. It is defined by

$$h_{\mathrm{R}} = m_{\mathrm{R}}^2 \frac{1}{N^3} \sum_{\alpha_1, \ldots, \alpha_6} \Gamma_{\mathrm{R}}^{(6)}(0, \ldots, 0)_{\alpha_1, \ldots, \alpha_6} + 10 g_{\mathrm{R}}^2 \tag{24}$$

and is proportional to the connected six-point-function at zero momentum. In perturbation theory one obtains in the infinite volume

$$h_R = 10g_R^2 - 15g_R^3 m_R^2 \frac{N+26}{27} J_3(m_R, \infty)$$

$$+ \left(1.3193(N-1) + \frac{45}{2}\right)\left(\frac{g_R}{4\pi}\right)^4 + \mathcal{O}\left(g_R^5, m_R^2 g_R^4\right). \tag{25}$$

The first two terms are from lattice one-loop perturbation theory, whereas the last term, taken from ref. [7], is the two-loop contribution in the continuum, i.e. neglecting scaling violations.

The finite size effect on h_R is in the notation of eq. (13) given by

$$\delta h_R = -15g_R^3\left(2\frac{N+8}{9}\delta J_2 + m_R^2 \frac{N+26}{27}\delta J_3\right) + \mathcal{O}\left(g_R^4\right). \tag{26}$$

3. Results of the numerical simulation

As already mentioned in sect. 1, the simulations in the O(4)-symmetric model were done using partly the conventional Metropolis algorithm, with two hits per sweep and one measurement after every fourth sweep, and partly a cluster algorithm, where the number of measurements and the number of sweeps are identical. The Metropolis algorithm was applied to $L^3 \times 12$ lattices with $L = 4, 6, 8, 10, 12$ at $\kappa = 0.290$, whereas the cluster algorithm was used for $L^3 \times 16$ lattices with $L = 8, 10, 12, 14, 16$ at $\kappa = 0.297$. In order to get precise values in the large volume limit at $\kappa = 0.290$ an additional run with the cluster algorithm was made on a 12^4 lattice.

3.1. REFLECTION CLUSTER ALGORITHM

Cluster algorithms have been applied previously to different scalar theories, see refs. [8–11]. In particular, numerical aspects of the cluster algorithm used in this work are presented in ref. [12]. Therefore, only a very short description will be given here. A more detailed description can be found in ref. [11].

The cluster algorithm used in this investigation consists of four steps:

- choose a random direction $r \in O(4)$;
- build clusters c by putting bonds between adjacent spins ϕ_x and ϕ_y with a certain probability p

$$p = 1 - \exp\left(\min\left(0, -4\kappa r^\alpha \phi_x^\alpha r^\beta \phi_y^\beta\right)\right);$$

- choose randomly a subset of these clusters with probability $1/2$;
- reflect the spins in this subset with respect to the hyperplane perpendicular to r.

One site update with this cluster algorithm takes 7 μs, which corresponds to 3–4 Metropolis updates. But the cluster algorithm has much shorter autocorrelation times and, by using so-called cluster observables for variance reduction, one can achieve a saving of CPU time of about a factor 10–100 depending on the quantity chosen for measurement. In the reflection algorithm most of the program is fully vectorized and only the cluster search part has not been vectorized for clusters with more than two spins. The identification of the one- and two-point clusters, however, has been vectorized.

3.2. ONE-PARTICLE MASSES

Using the correlation function

$$G(t) = \frac{1}{N}\frac{1}{L^6}\left\langle \sum_{x,y} \phi^{\alpha}_{t,x}\phi^{\alpha}_{0,y} \right\rangle \tag{27}$$

the one-particle mass m is determined by means of a conventional fit

$$G(t) = c_1(\mathrm{e}^{-mt} + \mathrm{e}^{-m(T-t)}). \tag{28}$$

In addition we define effective masses by solving eq. (28) for different pairs of time-slices during the run. This allows a more accurate estimation of the errors of the fit parameters, because the time-slices of the correlation function are highly correlated and therefore there is no simple way to determine the error of the mass from the errors of the correlation function. The corresponding cluster observable is defined as follows:

$$G(t) = \frac{1}{L^6}\left\langle \sum_{c}\sum_{x,y} r^{\alpha}\phi^{\alpha}_{t,x} r^{\beta}\phi^{\beta}_{0,y}\Theta(t,\boldsymbol{x};c)\Theta(0,\boldsymbol{y};c) \right\rangle \tag{29}$$

with

$$\Theta(x;c) = \Theta(t,\boldsymbol{x};c) = \begin{cases} 1 & \text{if } x = (t,\boldsymbol{x}) \in c \\ 0 & \text{otherwise} \end{cases}. \tag{30}$$

It allows a determination of the mass, which is more precise by a factor 8–10.

3.3. TWO-PARTICLE MASSES

Using the operator $S^{\alpha\beta}(t)$ defined in eq. (18) we get for the scalar 1-dimensional representation

$$G_1(t) = \langle S^{\alpha\alpha}(t) S^{\beta\beta}(0) \rangle \tag{31}$$

and for the tensorial 9-dimensional representation

$$G_9(t) = \left\langle \left(S^{\alpha\beta}(t) - \tfrac{1}{4} S^{\gamma\gamma}(t)\delta^{\alpha\beta} \right) \left(S^{\beta\alpha}(0) - \tfrac{1}{4} S^{\delta\delta}(0)\delta^{\beta\alpha} \right) \right\rangle . \tag{32}$$

By means of a fit

$$G(t) = c_0 + c_1 (\mathrm{e}^{-Mt} + \mathrm{e}^{-M(T-t)}) \tag{33}$$

the masses M_1 and M_9, belonging to the two possible two-particle scattering states for zero relative momentum are extracted.

The cluster observables always measure the correlations between the components of the spins in the direction of r. Since this projection mixes the two-particle states, they can only provide a reducible combination and the extraction of useful physical information is difficult. Therefore, the two-particle correlations have not been considered in cluster observables.

3.4. n-POINT FUNCTIONS

The non-connected n-point functions at zero momentum can be defined in the spin representation as

$$\varphi_n = \frac{1}{N^{n/2}} \frac{1}{V} \left\langle \left(\sum_{x,\alpha} \phi_x^\alpha \right)^n \right\rangle . \tag{34}$$

$V = L^3 T$ is the total lattice volume. However, we realized that for the determination of the non-connected n-point functions it is more convenient to use the following quantities:

$$\bar{\varphi}_n = \frac{1}{N^{n/2}} \frac{1}{V} \left\langle \left(\sum_{x,y} \phi_x^\alpha \phi_y^\alpha \right)^{n/2} \right\rangle . \tag{35}$$

Various correlations of different spin components, which average to zero because of the O(N)-symmetry, have disappeared. The $\bar{\varphi}_n$ are related to the original quantities by certain group theoretical factors, e.g.

$$\varphi_2 = \bar{\varphi}_2 , \qquad \varphi_4 = \frac{3N}{(N+2)} \bar{\varphi}_4 , \qquad \varphi_6 = \frac{3N}{(N+2)} \frac{5N}{(N+4)} \bar{\varphi}_6 . \tag{36}$$

The corresponding connected n-point functions, the susceptibilities χ_n, which are needed for information on the physical couplings, are defined in the symmetric phase as usual by

$$\chi_2 = \varphi_2 , \qquad \chi_4 = \varphi_4 - 3V(\varphi_2)^2 , \qquad \chi_6 = \varphi_6 - 15V\varphi_2\varphi_4 + 30V^2(\varphi_2)^3 . \tag{37}$$

Finally, the cluster representations of the n-point functions are as follows. Defining the quantity $s(c)$ through

$$s(c) = \sum_x r^{\alpha} \phi_x^{\alpha} \Theta(x; c) \tag{38}$$

we have

$$\varphi_2 = \frac{1}{V} \left\langle \sum_c s^2(c) \right\rangle,$$

$$\varphi_4 = -\frac{2}{V} \left\langle \sum_c s^4(c) \right\rangle + \frac{3}{V} \left\langle \left(\sum_c s^2(c) \right)^2 \right\rangle,$$

$$\varphi_6 = \frac{16}{V} \left\langle \sum_c s^6(c) \right\rangle - \frac{30}{V} \left\langle \left(\sum_c s^4(c) \right) \left(\sum_c s^2(c) \right) \right\rangle + \frac{15}{V} \left\langle \left(\sum_c s^2(c) \right)^3 \right\rangle. \tag{39}$$

3.5. RENORMALIZED QUANTITIES

From the measured values of the mass m and the susceptibilities χ_2, χ_4 and χ_6 the renormalized mass m_R, the wave function renormalization Z_R and the couplings g_R and h_R are obtained in the following way (see also ref. [8]). We define

$$\lambda_n = m^{2n-4} \frac{\chi_n}{(\chi_2)^{n/2}}. \tag{40}$$

These quantities are dimensionless and the wave function renormalization cancels out in them. With the mass ratio

$$r = m_R/m \tag{41}$$

we have the relations

$$g_R = -r^4 \lambda_4, \qquad h_R = r^8 \lambda_6, \qquad Z_R = 2\kappa r^2 m^2 \chi_2, \qquad m_R = rm. \tag{42}$$

The ratio $r(L)$ is close to 1 (a typical value is $r \approx 1.004$ at $\kappa = 0.297$) and its numerical value can be obtained from one-loop lattice perturbation theory, eqs. (13) and (14), with sufficient accuracy. This allows us to determine the remaining quantities from the Monte Carlo results using eqs. (42).

3.6. RESULTS

The results of our numerical simulations are collected in tables 1–4. Table 3 contains an explicit comparison of the three different methods of measuring the non-connected n-point functions discussed in subsect. 3.4. They exhibit the

TABLE 1
The measured quantities at $\kappa = 0.290$ for different lattices $L^3 \times 12$

L	Ms	χ_2	$-\chi_4$	χ_6	m	M_1	M_9
4	4	5.44(2)	0.54(2)E4	0.37(2)E8	0.548(4)	1.380(8)	1.179(3)
6	4	7.54(3)	0.21(2)E5	0.54(12)E9	0.468(5)	1.064(7)	0.974(4)
8	4	8.18(3)	0.37(3)E5	0.13(11)E10	0.451(5)	0.960(6)	0.922(4)
10	4	8.34(4)	0.30(10)E5	0.48(58)E10	0.447(6)	0.918(8)	0.902(5)
12	4	8.43(4)	0.26(20)E5	−0.10(17)E11	0.447(6)	0.904(8)	0.898(5)
12*	0.5	8.40(1)	0.46(4)E5	0.12(20)E10	0.4465(6)	0.91(1)	0.898(8)

The simulations were done with a Metropolis algorithm. χ_2, χ_4, χ_6 are the susceptibilities, obtained according to eqs. (34) and (37), m is the one-particle mass, M_1 and M_9 are the two-particle masses in the 1- and 9-representation. Ms means the number of million sweeps. The last row marked with a star is a run with the cluster algorithm.

superiority of the cluster observables, which are therefore used for computing the physical quantities in table 4. The volume dependence of the physical mass m and coupling g_R on the $T = 16$ lattices is also shown in fig. 1 and fig. 2, respectively. The extrapolation of the renormalized mass and coupling to infinite volume was done both in table 2 and table 4 by matching the values of the Monte Carlo analysis and of perturbation theory on the largest (T^4) lattice. The perturbative finite volume behaviour of the six-point coupling h_R was obtained by taking the infinite volume limit from perturbation theory, eq. (25), and adding the one-loop finite volume corrections on the lattice, eq. (26). As can be seen from the tables and figures, the finite size effects are well reproduced by one-loop lattice perturbation

TABLE 2
The renormalized physical quantities at $\kappa = 0.290$ derived from table 1 as explained in subsect. 3.5

L	m_R	g_R	h_R	Z_R	m_{PT}	g_{PT}	h_{PT}
4	0.555(4)	17(1)	0.21(2)E4	0.97(2)	0.657	–	–
6	0.472(5)	19(2)	0.31(7)E4	0.98(3)	0.483	16.1	–
8	0.455(5)	24(7)	0.43(37)E4	0.98(2)	0.457	23.9	0.416E4
10	0.450(6)	18(8)	–	0.98(3)	0.452	25.9	0.578E4
12	0.450(6)	16(10)	–	0.99(3)	0.450	26.6	0.630E4
12*	0.4502(6)	26.6(2.1)	–	0.988(2)	0.450	26.6	0.630E4
∞					0.450	26.9	0.659E4

m_R is the renormalized mass, g_R and h_R the renormalized 4- and 6-point couplings, Z_R the wave function renormalization. m_{PT}, g_{PT} and h_{PT} are the values of m_R, g_R and h_R from finite size perturbation theory. A dash (–) means that either the measured errors are too large or that finite size perturbation theory yields negative values due to a volume which is too small. The extrapolated values of m_R, g_R and h_R at infinite volume are shown in the last row.

TABLE 3
The measured quantities at $\kappa = 0.297$ for different lattices $L^3 \times 16$

L	Ms	χ_2	$-\chi_4$	χ_6	m	M_1	M_9
8	0.4	15.66(10)	0.32(2)E6	0.49(22)E11	0.328(4)	0.73(1)	0.68(1)
10	0.4	16.84(10)	0.46(6)E6	0.78(86)E11	0.307(4)	0.67(1)	0.63(1)
12	0.4	17.46(10)	0.69(11)E6	0.12(30)E12	0.306(4)	0.64(1)	0.63(1)
14	0.6	17.60(8)	0.60(14)E6	0.55(82)E12	0.307(3)	0.63(1)	0.61(1)
16	0.5	17.69(8)	0.64(23)E6	0.02(16)E13	0.306(3)	0.61(1)	0.61(1)
L	Ms	χ_2	$-\chi_4$	χ_6			
8	0.4	15.67(8)	0.35(2)E6	0.60(5)E11			
10	0.4	16.80(7)	0.53(3)E6	0.16(3)E12			
12	0.4	17.36(7)	0.62(6)E6	0.15(10)E12			
14	0.6	17.70(6)	0.79(10)E6	0.09(20)E12			
16	0.5	17.73(6)	0.77(11)E6	−0.01(45)E12			
L	Ms	χ_2	$-\chi_4$	χ_6	m		
8	0.4	15.64(5)	0.34(1)E6	0.61(4)E11	0.3244(7)		
10	0.4	16.84(5)	0.55(2)E6	0.13(2)E12	0.3107(7)		
12	0.4	17.41(4)	0.68(4)E6	0.22(7)E12	0.3069(6)		
14	0.6	17.64(3)	0.79(4)E6	0.25(14)E12	0.3052(4)		
16	0.5	17.75(3)	0.80(6)E6	0.66(26)E12	0.3039(4)		

The simulations were done with the cluster algorithm. The notation is as in table 1. In the first part the n-point functions are measured with the help of eq. (34), whereas in the second part they are determined via eq. (35). In the third part the corresponding values from the cluster representation are given.

TABLE 4
The renormalized physical quantities at $\kappa = 0.297$ derived from the third part of table 3. The notation is as in table 2

L	m_R	g_R	h_R	Z_R	m_{PT}	g_{PT}	h_{PT}
8	0.3258(7)	15.6(0.5)	0.20(3)E4	0.986(5)	0.3333	11.3	–
10	0.3120(7)	18.5(0.8)	0.24(4)E4	0.973(4)	0.3140	17.9	0.175E4
12	0.3081(6)	20.3(1.2)	0.34(6)E4	0.982(3)	0.3080	20.4	0.333E4
14	0.3064(4)	22.2(1.1)	0.35(19)E4	0.984(2)	0.3058	21.5	0.401E4
16	0.3050(4)	21.9(1.7)	0.88(35)E4	0.981(2)	0.3050	21.9	0.431E4
∞					0.3044	22.4	0.461E4

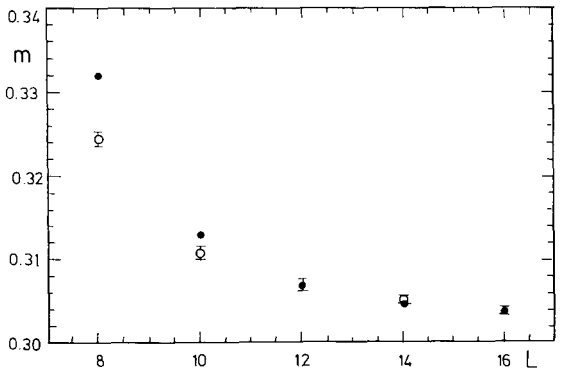

Fig. 1. The dependence of the one-particle mass m on the space extension L of the $L^3 \cdot T$ lattice with $T = 16$ at $\kappa = 0.297$. The open circles are the measured values, the full circles the results of one-loop lattice perturbation theory.

theory. Therefore, the extrapolation to infinite volume is on firm ground. The infinite volume results agree well with the analytical results of Lüscher and Weisz [7], as is shown for instance for the renormalized coupling g_R in fig. 3. In this figure are also shown the results of a previous numerical simulation at infinite bare quartic coupling [5], which agree within errors with ref. [7] and with our results. The fit curve in ref. [5] is actually somewhat lower than our points, but in this global fit different lattice sizes at different λ-values are included for two different definitions of the finite size couplings (which can have different finite size effects).

As we discussed in sect. 2, the measured values of the two-particle masses M_1 and M_9 can be used to determine the scattering lengths in the O(4) scalar and tensor channels respectively. The values of $(M_{1,9} - 2m)$ were fitted as a function of L with

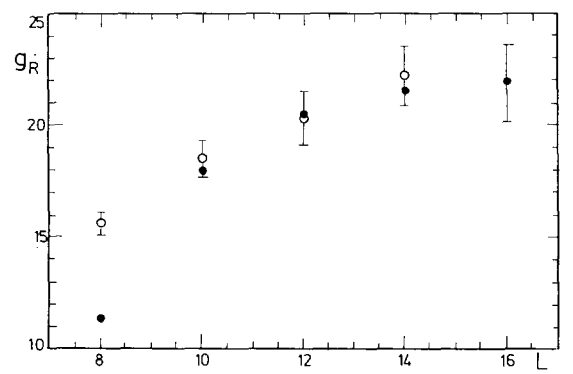

Fig. 2. The dependence of the renormalized coupling g_R on the space extension L of the $L^3 \cdot T$ lattice with $T = 16$ at $\kappa = 0.297$. The open circles are the measured values, the full circles the results of one-loop lattice perturbation theory.

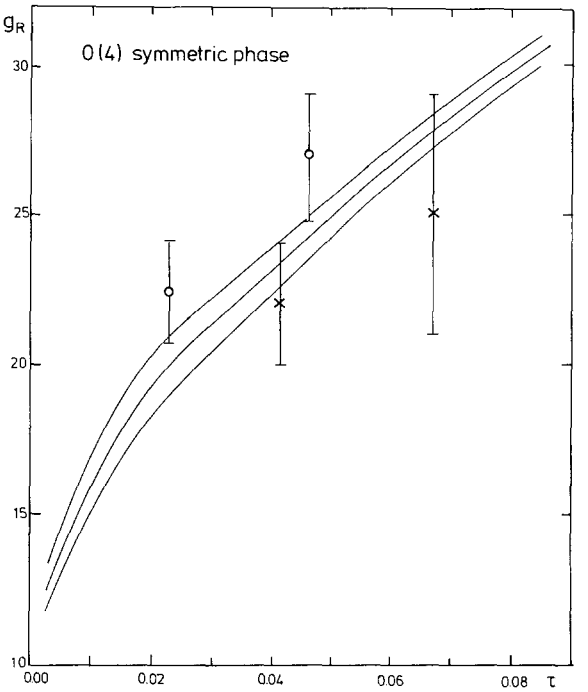

Fig. 3. Comparison of our results (open circles) to the analytical work in ref. [7] (strip given by three lines) and to the numerical results of ref. [5]. The renormalized coupling g_R is shown as a function of $\tau = 1 - \kappa/\kappa_c$ with $\kappa_c \equiv 0.30411$.

TABLE 5
The S-wave scattering lengths a_0^s and a_0^t for $\kappa = 0.290$ and $\kappa = 0.297$

	$\kappa = 0.290$	$\kappa = 0.297$
$-a_0^s$	0.74(10)	0.92(7)
	0.89(7)	1.14(9)
$-a_0^t$	0.32(7)	0.46(7)
	0.35(7)	0.44(3)

The upper number in each entry results from a fit of the mass differences $M_{1,9} - 2m$ as a function of L according to eq. (15), the lower numbers are the predictions from the perturbation theory, eqs. (19) and (20).

formula (15) in order to obtain the scattering lengths $a_0^{s,t}$. The results of this fit together with a comparison with the perturbative two-loop formulae (19) and (20) are contained in table 5. Although the errors are not very small, the overall agreement is remarkable, showing that the lattices considered in this paper are large enough in order to contain also the lowest two-particle states in a relatively undistorted form. In other words, information about low-energy scattering can be obtained from these lattice studies, similarly to the case of a single-component ϕ^4-theory [8].

4. Summary and conclusions

The results of our numerical simulations of the O(4)-symmetric ϕ^4-theory in the symmetric phase fit well into the recently emerging picture of the behaviour of lattice ϕ^4-models at maximal (infinite) bare self-coupling [3–9]. In the scaling region near the critical point the renormalized coupling is always small enough for the applicability of renormalized perturbation theory. In particular, the finite volume dependence of the physical quantities is well reproduced and hence is fully under control. This allows for a reliable infinite volume extrapolation. Moreover, a careful study of the finite size effects yield useful physical information, for instance, on low-energy scattering. In this respect there is qualitatively very little difference between the four-component model and the previously studied single-component case [8].

An important aspect is the comparison to the analytical calculation based on 14th order hopping parameter expansion and three-loop perturbative renormalization group equations [7]. In general, there is good agreement between the results of ref. [7] and our numerical simulation. The estimated relative errors in the renormalized mass are up to a factor of 5–10 smaller in the numerical simulation but, as is shown by fig. 3, the errors of the renormalized coupling are somewhat worse here, in spite of the use of the cluster algorithm. Since the total computer time used in this project was about 550 CPU-hours on a CRAY X-MP, where 300 hours have been spent for the calculation with the Metropolis algorithm, a really large scale numerical calculation by present day standards could, in principle, beat the analytical calculation also in the error of the renormalized coupling.

The Monte Carlo calculations for this investigation have been performed on the CRAY X-MP/416 of HLRZ, Jülich.

References

[1] R. Dashen and H. Neuberger, Phys. Rev. Lett. 50 (1983) 1987
[2] I. Montvay, Phys. Lett. B172 (1986) 71; Nucl. Phys. B293 (1987) 479
[3] A. Hasenfratz, K. Jansen, C.B. Lang, T. Neuhaus and H. Yoneyama, Phys. Lett. B199 (1987) 531; A. Hasenfratz, K. Jansen, J. Jersák, C.B. Lang, T. Neuhaus and H. Yoneyama, Nucl. Phys. B317 (1989) 81;

K. Jansen, Nucl. Phys. B (Proc. Suppl.) 4 (1988) 422;
C.B. Lang, in Lattice Higgs Workshop, ed. B. Berg et al. (World Scientific, Singapore, 1988) p. 158;
T. Neuhaus, Nucl. Phys. B (Proc. Suppl.) 9 (1989);
A. Hasenfratz, K. Jansen, J. Jersák, C.B. Lang, H. Leutwyler and T. Neuhaus, preprint FSU-SCRI-89-42, BI-TP 89/08

[4] J. Kuti, L. Lin and Y. Shen, Nucl. Phys. B (Proc. Suppl.) 4 (1988) 397; Phys. Rev. Lett. 61 (1988) 678;
J. Kuti, L. Lin, Y. Shen and S. Meyer, in Lattice Higgs Workshop, ed. B. Berg et al. (World Scientific, Singapore, 1988) p. 216;
J. Kuti, in Proc. XXIV Int. Conf. on HEP, Munich 1988, ed. R. Kotthaus and J.H. Kühn (Springer, 1989)

[5] J. Kuti, L. Lin and Y. Shen, in Lattice Higgs Workshop, ed. B. Berg et al. (World Scientific, Singapore, 1988), p. 140

[6] M. Lüscher and P. Weisz, Nucl. Phys. B290 [FS20] (1987) 25; B295 [FS21] (1988) 65; Phys. Lett. B212 (1988) 472

[7] M. Lüscher and P. Weisz, Nucl. Phys. B318 (1989) 705

[8] I. Montvay and P. Weisz, Nucl. Phys. B290 [FS20] (1987) 327;
I. Montvay, G. Münster and U. Wolff, Nucl. Phys. B305 [FS23] (1988) 143

[9] K. Jansen, J. Jersák, I. Montvay, G. Münster, T. Trappenberg and U. Wolff, Phys. Lett. B213 (1988) 203;
K. Jansen, I. Montvay, G. Münster, T. Trappenberg and U. Wolff, Nucl. Phys. B322 (1989) 698

[10] F. Niedermayer, Phys. Rev. Lett. 61 (1988) 2026

[11] U. Wolff, Phys. Rev. Lett. 62 (1989) 361; Nucl. Phys. B322 (1989) 759; preprint DESY 89-021

[12] Ch. Frick, K. Jansen and P. Seuferling, preprint HLRZ 89-38

[13] M. Lüscher, Comm. Math. Phys. 105 (1986) 153